催化学报
2012 Chinese Journal of Catalysis Vol. 33 No. 8

文章编号: 0253-9837(2012)08-1334-06 国际版 DOI: 10.1016/S1872-2067(11)60408-7 研究论文: 1334~1339

三维花状 Co_3O_4 的低成本制备及其在催化 CO 氧化中的应用

曹昌燕, 窦智峰, 刘 华, 宋卫国*

中国科学院化学研究所, 北京分子科学国家实验室, 分子纳米结构与纳米技术实验室, 北京 100190

摘要: 采用一种快速、无模板、低成本的微波辅助水热法在 2 min 内制备了三维花状 Co_3O_4. 所用原料均是无机盐. 前驱体浓度和尿素的逐渐水解对 Co_3O_4 形貌影响很大. 制得的花状 Co_3O_4 比表面积大, 且暴露了 (110) 高活性指数面, 对 CO 氧化具有较高的催化活性.

关键词: 一氧化碳; 氧化; 四氧化三钴; 纳米结构; 微波

中图分类号: O643 **文献标识码**: A

收稿日期: 2012-03-24. 接受日期: 2012-05-07.

*通讯联系人. 电话/传真: (010)62557908; 电子信箱: wsong@iccas.ac.cn

基金来源: 国家重点基础研究发展计划 (973 计划, 2009CB930400, 2011CB933700); 国家自然科学基金 (21121063).

本文的英文电子版(国际版)由Elsevier出版社在ScienceDirect上出版(http://www.sciencedirect.com/science/journal/18722067).

Low Cost Synthesis of 3D Flowerlike Co_3O_4 Nanostructures as Active Catalyst for CO Oxidation

CAO Changyan, DOU Zhifeng, LIU Hua, SONG Weiguo*

Beijing National Laboratory for Molecular Science (BNLMS), Laboratory of Molecular Nanostructures and Nanotechnology, Institute of Chemistry, Chinese Academy of Sciences, Beijing 100190, China

Abstract: 3D flowerlike Co_3O_4 nanostructures were prepared by a microwave-assisted hydrothermal method, which is a rapid, template-free, and low cost method. The product is obtained in two minutes using all inorganic precursors. The precursor concentration and gradual hydrolysis of urea determine the morphology of Co_3O_4 nanostructures. These flowerlike Co_3O_4 nanostructures have high surface area and expose largely active (110) planes, leading to relative high catalytic activity in CO oxidation.

Key words: carbon monoxide; oxidation; cobaltosic oxide; nanostructure; microwave

Received 24 March 2012. Accepted 7 May 2012.

**Corresponding author. Tel/Fax: +86-10-62557908; E-mail: wsong@iccas.ac.cn*

This work was supported by the National Basic Research Program of China (973 Program, 2009CB930400 and 2011CB933700) and the National Natural Science Foundation of China (21121063).

English edition available online at Elsevier ScienceDirect (http://www.sciencedirect.com/science/journal/18722067).

Cobalt oxide (Co_3O_4) nanomaterials are widely used in heterogeneous catalysts, chemical sensors, lithium-ion batteries, and magnetic materials [1–14]. Various Co_3O_4 structures such as nanoparticles [4], nanocubes [1,15], nanorods [2,3], nanosheets [1], nanowires [16], hollow spheres, and flowerlike nanostructures [17–20] have been synthesized by a variety of methods. Their properties in these applications strongly depend on their sizes and morphologies. In particular, three-dimensional (3D) flowerlike Co_3O_4 nanostructures are composed of nanosized building blocks while their total sizes are in micrometer scale. Such hierarchical structures possess advantages of both microstructures and nanostructures, i.e. large surface area, facile mass transportation, and easiness to recycle, making them ideal materials for catalysis.

Soft templates (surfactants) are frequently used to prepare 3D flowerlike nanostructures [21–26]. However, expensive organic surfactants, and in many cases organic cobalt precursors and organic solvent (ethylene glycol (EG)) are needed in these ployol mediated methods. Removing these

templates adds another time consuming and costly calcination step. It will be very desirable for the practical application of flowerlike Co_3O_4 nanostructures if they can be produced by a reliable, low cost, and template-free method in aqueous medium.

The microwave assisted hydrothermal method is a reliable and rapid method to produce nanomaterials, including CeO_2 hollow nanospheres [27] and flowerlike NiO hollow nanospheres [28]. In this study, flowerlike Co_3O_4 nanostructures were produced using cobalt chloride and urea as raw materials, and water as solvent. Unlike previously reported EG-mediated methods for flowerlike nanostructures [24–26], no organic template, organic metal compounds or organic solvent was used. All chemicals used were low cost inorganic compounds and environmentally benign. The synthesis reaction time was completed in less than 2 min with microwave heating. These make this aqueous route a rapid, reliable and low cost method that can be scaled up in practical uses. These 3D flowerlike Co_3O_4 nanostructures had high surface area with largely active (110) planes being exposed, showing relatively high catalytic activity in CO oxidation. CO conversion reached 100% at 60 °C.

1 Experimental

1.1 Preparation of flowerlike Co_3O_4 nanostructures

In a typical procedure, 1 mmol $CoCl_2·6H_2O$ (Beijing Chemicals Co.) and 1.5 mmol urea (Beijing Chemicals Co.) were dissolved in 100 ml deionized water, and then the reaction solution was poured into a Teflon-lined autoclave. The autoclave was sealed and placed in a programmable microwave oven (MDS-6, Shanghai Sineo Microwave Chemistry Technology Co., Ltd.). The oven was heated to 170 °C in 2 min by microwave irradiation and then kept at that temperature for another 2 min. After cooling to room temperature, precipitates were collected as Co_3O_4 precursors by centrifugation and washed with water and ethanol three times, respectively. Co_3O_4 was obtained after calcination of the precursors in air at 200 °C for 4 h. Compared with the preparation of flowerlike Co_3O_4, Co_3O_4 nanosheets were obtained using NaOH as alkali instead of urea with other conditions unchanged. While Co_3O_4 nanowires can be obtained when the reaction concentration was magnified 5 times.

1.2 Characterization

X-ray diffraction (XRD) patterns were obtained on a Rigaku D/max-2500 diffractometer with Cu K_α radiation (λ = 0.15418 nm) at 40 kV and 200 mA. The morphology and microstructures of the samples were characterized by field emission scanning electron microscopy (FE-SEM, JOEL 6701F), transmission electron microscopy (TEM, JEOL 1011), and high-resolution transmission electron microscopy (HR-TEM, FEI Tecnai F20). The nitrogen adsorption-desorption isotherms were measured on a Quantachrome Autosorb AS-1 instrument. The pore size distributions were derived from the desorption branches using the Barrett-Joyner-Halenda (BJH) model. H_2 temperature-programmed reduction (H_2-TPR) of different cobalt oxides was performed using 10% H_2 in N_2 as the reducing gas. The flow rate of H_2/N_2 was adjusted by mass flow controller under 25 ml/min. The cell was a quartz tube with an inner diameter 8 mm and 50 mg of the catalyst was mounted with quartz wool. The hydrogen consumption was monitored by a thermal conductivity detector (TCD) on raising the sample temperature from room temperature to 500 °C at a constant rate of 5 °C/min.

1.3 CO oxidation test

CO oxidation test was performed in a quartz tubular reactor (7 mm inside diameter) loaded with 50 mg Co_3O_4 and 450 mg sea sand. The catalyst was activated first in air flow (25 ml/min) at 200 °C for 1 h. The CO oxidation test was carried out with 25 sccm flow of 1% CO in nitrogen and 25 sccm (80% N_2 + 20% O_2). The gas composition was monitored by online gas chromatography (Shimadzu, GC-14C).

2 Results and discussion

2.1 Characterizations of flowerlike Co_3O_4 nanostructures

Figure 1(a) shows the low-magnification SEM image of typical Co_3O_4 precursors after microwave heating. They were composed of flowerlike architectures approximately 2–3 μm in diameter. A closer examination by high-magnification SEM (Fig. 1(b)) indicated that the entire structure of the architecture was built of many nanopetals. These nanopetals were ca. 60 nm thick and 1 μm wide, and connected to each other to form 3D flowerlike structures. The TEM image (Fig. 1(c)) further confirmed the flowerlike structures, which were similar to previously reported iron oxide and ceria structures [24,25]. The powder XRD pattern of the typical precursor is shown in Fig. 2(1). The main diffraction peaks can be indexed to the hexagonal phase of $Co(OH)_2$ (JCPDS 51-1731) and cubic phase of Co_3O_4 (JCPDS 43-1003). The whole reaction processes can be illustrated by following equations (1)–(4):

$$CO(NH_2)_2 + H_2O \rightarrow 2NH_3 + CO_2 \quad (1)$$

$$NH_3 + H_2O \rightarrow NH_4^+ + OH^- \quad (2)$$

$$Co^{2+} + 2OH^- \rightarrow Co(OH)_2 \quad (3)$$

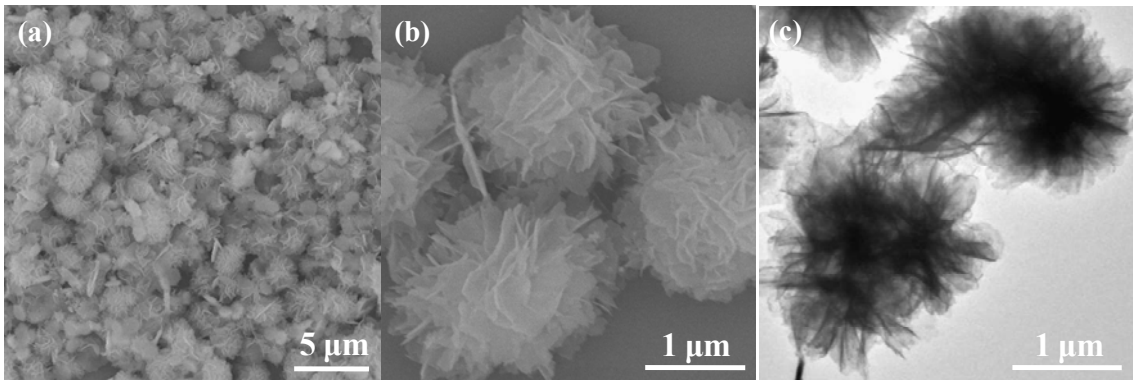

Fig. 1. Low-magnification (a) and high-magnification (b) SEM images and TEM image (c) of flowerlike Co_3O_4 nanostructure precursors.

$$6Co(OH)_2 + O_2 \rightarrow 2Co_3O_4 + 6H_2O \quad (4)$$

After being calcined at 200 °C for 4 h in air, the precursors were transformed to pure phase Co_3O_4. The XRD pattern of calcined product (Fig. 2(2)) matched well with the standard PDF card (JCPDS 43-1003). The broaden diffraction peaks indicated the small size of nanocrystal building blocks. The TEM image in Fig. 3(a) shows a very similar flowerlike morphology, indicating that calcination did not change the total morphology of Co_3O_4. High-magnification TEM image (inset in Fig. 3(a)) showed that the nanopetals were composed of loose nanoparticles. The lattice fringes in the HR-TEM image (Fig. 3(b)) showed a spacing of 0.47 nm due to the (111) planes and a spacing of 0.28 nm from the (220) planes of cubic Co_3O_4.

The nitrogen adsorption-desorption isotherm of flowerlike Co_3O_4 is shown in Fig. 4. The specific surface area of flowerlike Co_3O_4 was 113 m^2/g calculated from the adsorption isotherm. Such high surface area was unusual for metal oxide and may be ascribed to the particular flowerlike hierarchical nanostructures. Two pore size distributions with average pore diameters of 4.2 and 17.6 nm were obtained by the BJH method. These pores were very likely due to the void spaces of stacked nanoparticles and curled nanopetals.

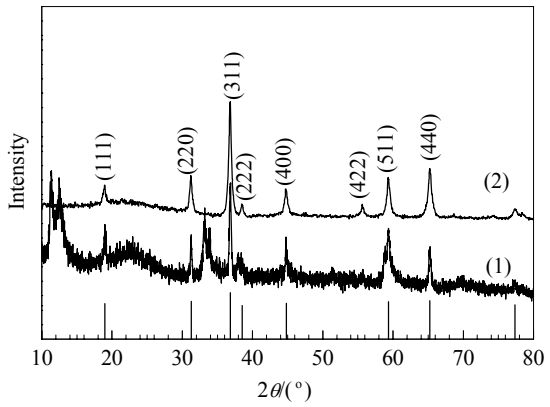

Fig. 2. XRD patterns of flowerlike Co_3O_4 precursors (1) and flowerlike Co_3O_4 nanostructures (2).

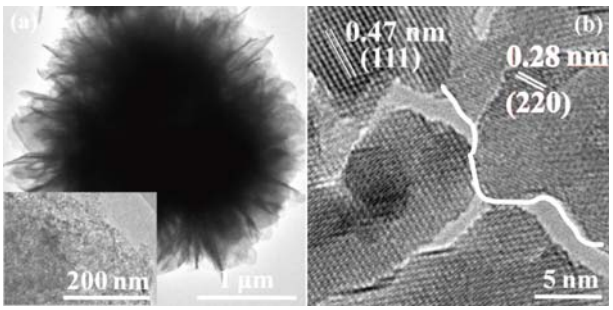

Fig. 3. TEM (a) and HR-TEM (b) images of flowerlike Co_3O_4 nanostructures.

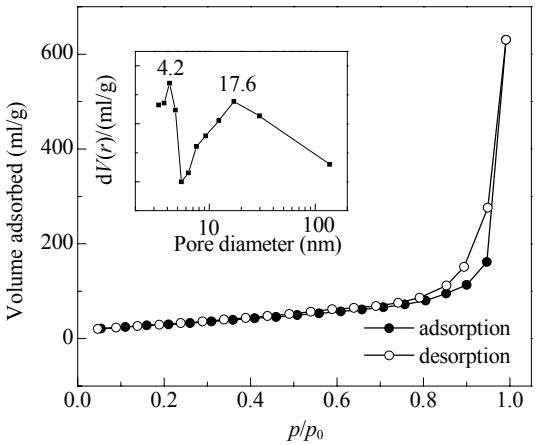

Fig. 4. Nitrogen adsorption-desorption isotherm (with the pore size distribution plot in the inset) of flowerlike Co_3O_4 nanostructures.

2.2 Formation mechanism of flowerlike Co_3O_4 nanostructures

In order to investigate the forming process of flowerlike Co_3O_4 precursors, samples prepared at different reaction times were collected and investigated by SEM (Fig. 5). Disc like nanoplates were immediately formed when the temperature reached 170 °C (Fig. 5(a)). The samples collected 1 min later showed nanopetals as well as flowerlike nanos-

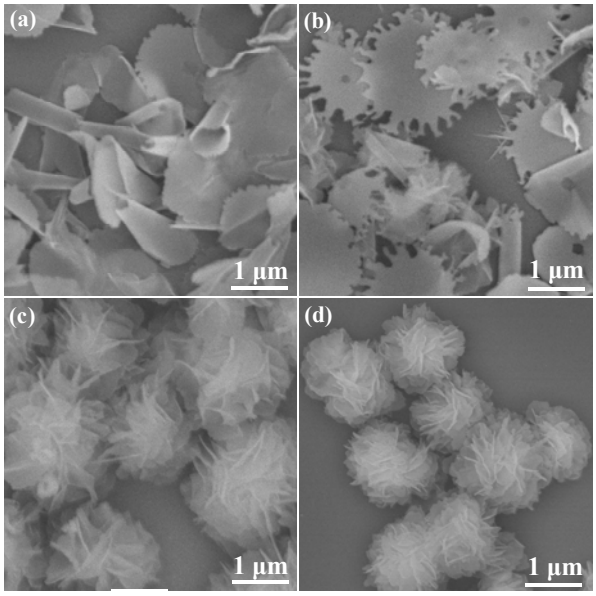

Fig. 5. SEM images of Co_3O_4 precursors obtained at different reaction times after temperature reached 170 °C. (a) 0 min; (b) 1 min; (c) 2 min; (d) 5 min.

tructures (Fig. 5(b)). As the reaction proceeded, all the samples became flowerlike structures with diameter of 2–3 μm after 2 min (Fig. 5(c)). From this point, the size and morphology of the product remained nearly the same with longer reaction times (Fig. 5(d)).

Common formation mechanism for such hierarchical nanostructures involved a two step growth model: fast nucleation of primary particles to form nanopetals through Ostwald-ripening followed by a self-assembly process [29]. However, Fig. 5 indicated that Co_3O_4 was very different from the previous reports on flowerlike α-Fe_2O_3 or MgO though the morphologies of these three metal oxides were similar. For flowerlike α-Fe_2O_3, amorphous spheres with smooth surface were first produced, and then the spheres changed into flowerlike crystalline structure; for flowerlike MgO, twisted crystalline ribbons (the building block for the whole flower like structure) were produced first, and then the ribbons assembled into flowerlike structure. However, for this flowerlike Co_3O_4, the starting building blocks seemed to be the disc like plates, which have similar XRD features as the final flowerlike structures. Shortened synthesis time (less than 1 min for disc like plates) also made it difficult to collect any species prior to the formation of nanoplates in Fig. 5(a). The flat disc started to roll and twist in Fig. 5(b). Further twisting and assembly led to flowerlike structures. Note that the yield of flat plates in Fig. 5(a) reached 100% based on the $CoCl_2·6H_2O$, thus the morphology evolution from Fig. 5(a) to 5(c) was not driven by the addition of new solid species. It was likely driven by the surface tension, as twisting and rolling decreased the overall surface tension of the materials.

In those studies using organic templates, a small amount of flowerlike nanostructure was usually observed when no organic template was added, suggesting that the role of organic templates was mostly to improve the uniform morphology of the products. However, the morphology of flowerlike Co_3O_4 nanostructures in this work was quite uniform, as shown in Fig. 1(a). Microwave heating may be crucial for such uniform morphology. Microwave heating provides a much faster heating rate than that by normal oven heating. Such fast wave heating may result in a fast hydrolysis of urea, fast Ostwald-ripening, and fast self-assembly.

Urea plays an essential role by providing a spatially uniform supply of OH^- ion source through hydrolysis [24,25,27]. The reaction between the Co^{2+} and OH^- ions was thus homogeneous within the whole reaction mixture. When sodium hydroxide or ammonia was used in place of urea, while other conditions were kept the same, hexagonal nanosheets as well as many nanoparticles were obtained (Fig. 6(a) and Fig. 6(b)). In addition, when urea concentration was high, nanowires were obtained (Fig. 6(c) and Fig. 6(d)).

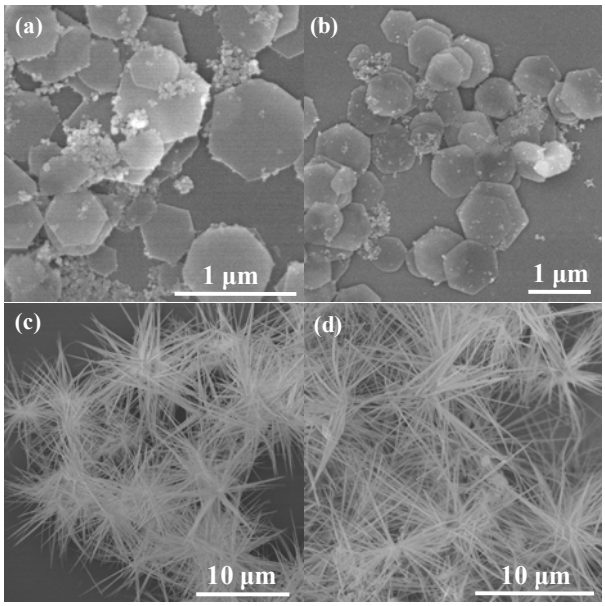

Fig. 6. SEM images of samples obtained using different alkali. (a) 1.5 mmol $NH_3·H_2O$; (b) 1.5 mmol NaOH; (c) 5 mmol urea; (d) 10 mmol urea.

2.3 Catalytic activity of flowerlike Co_3O_4 nanostructures for CO oxidation

CO oxidation is not only important in fuel cell industry but also a standard test reaction for oxidation catalysts [1,2,10,11,30,31]. The catalytic activity of Co_3O_4 was controlled by two factors: the surface area and the planes exposed [1,2,15]. In order to illustrate the influence of mor-

phology and structure on the property, Co_3O_4 nanosheet and Co_3O_4 nanowire were also test for comparison. The HR-TEM images of Co_3O_4 nanosheet and Co_3O_4 nanowire are shown in Fig. 7. Only (111) planes were exposed for nanowire, while both (111) and (220) planes were exposed for nanosheet. Figure 8 shows the CO conversion as a function of temperature of the three different morphologies Co_3O_4. It can be seen that flowerlike Co_3O_4 had the highest catalytic activity. With flowerlike Co_3O_4 the CO conversion reached 100% at 60 °C. For Co_3O_4 nanosheet and Co_3O_4 nanowire, the temperatures of 100% CO oxidation were 100 and 130 °C, respectively.

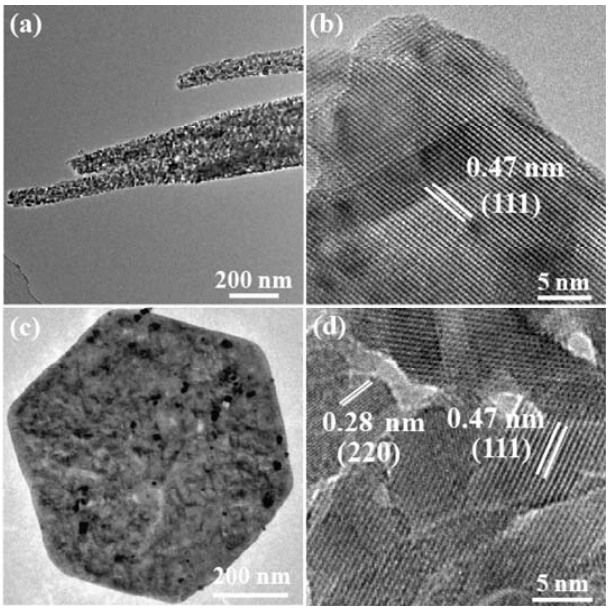

Fig. 7. TEM and HR-TEM images of Co_3O_4 nanowire (a, b) and Co_3O_4 nanosheet (c, d).

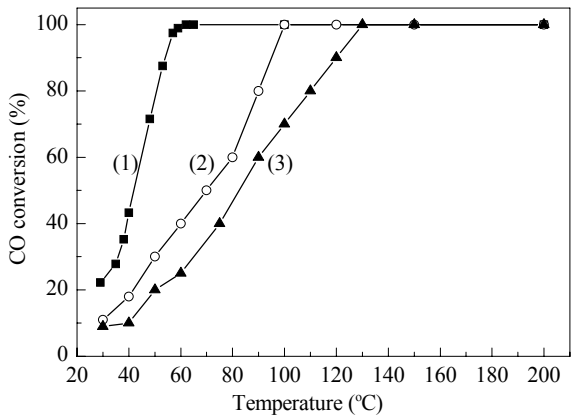

Fig. 8. CO conversion as a function of temperature for flowerlike Co_3O_4 (1), Co_3O_4 nanosheet (2), and Co_3O_4 nanowire (3).

Table 1 lists the surface area, planes exposed, and 100% CO conversion temperature of Co_3O_4 with different morphologies. For Co_3O_4 nanosheet and flowerlike Co_3O_4, because they exposed both (111) and (110) planes, the surface area might be the main factor for higher catalytic activity of the flowerlike Co_3O_4. However, Co_3O_4 nanosheet showed higher activity than the Co_3O_4 nanowires even though the latter had higher surface area, indicating that crystal planes were the decisive factor.

Table 1 Surface area, planes exposed, and 100% CO conversion temperature of flowerlike Co_3O_4, Co_3O_4 nanosheet, and Co_3O_4 nanowire

Catalyst	Surface area (m^2/g)	Plane exposed	100% CO conversion temperature (°C)
Flowerlike Co_3O_4	113	(111), (220)	60
Co_3O_4 nanosheet	40	(111), (220)	100
Co_3O_4 nanowire	49	(111)	130

As for Co_3O_4, theoretical studies have shown that (110) planes are significantly more active than (111) planes [2]. Therefore, the difference of catalytic activity between Co_3O_4 nanosheet and Co_3O_4 nanowire was mainly attributed to the exposed active planes. Flowerlike Co_3O_4 nanostructures not only had highest surface area but also exposed active planes, resulting in the highest catalytic activity.

Xie et al. [2] reported outstanding CO oxidation activity of Co_3O_4 nanorods with carefully controlled morphology with 41% of (110) facets being exposed. The activity of the flowerlike Co_3O_4 catalyst in this work was lower than that in Xie's work but was still relative high, as 100% CO conversion was reached at 60 °C. And the preparation method in this work was low cost as only $CoCl_2·6H_2O$, urea, and water were used, and all these raw materials were environmentally benign. The synthesis process was fast and ready to scale up. Thus for practical application, the flowerlike Co_3O_4 catalyst may have advantages.

3 Conclusions

A rapid and facile template-free microwave-assisted hydrothermal method was used to prepare flowerlike Co_3O_4 nanostructures. This was a low cost and environmentally benign method. The obtained flowerlike Co_3O_4 nanostructures had high surface area and exposed active (110) planes. As catalyst for CO oxidation, total CO conversion temperature was 60 °C.

References

1 Hu L H, Peng Q, Li Y D. *J Am Chem Soc*, 2008, **130**: 16136
2 Xie X W, Li Y, Liu Z Q, Haruta M, Shen W J. *Nature*, 2009, **458**: 746
3 Xie X W, Shang P J, Liu Z Q, Lv Y G, Li Y, Shen W J. *J Phys Chem C*, 2010, **114**: 2116
4 Xie R Y, Li D B, Hou B, Wang J A, Jia L T, Sun Y H. *Catal*

Commun, 2010, **12**: 380
5 Cao A M, Hu J S, Liang H P, Song W G, Wan L J, He X L, Gao X G, Xia S H. *J Phys Chem B*, 2006, **110**: 15858
6 Wang X, Wu X L, Guo Y G, Zhong Y T, Cao X Q, Ma Y, Yao J N. *Adv Funct Mater*, 2010, **20**: 1680
7 Li W Y, Xu L N, Chen J. *Adv Funct Mater*, 2005, **15**: 851
8 Barakat M N A, Khil M S, Sheikh F A, Kim H Y. *J Phys Chem C*, 2008, **112**: 12225
9 Wang G X, Shen X P, Horvat J, Wang B, Liu H, Wexler D, Yao J. *J Phys Chem C*, 2009, **113**: 4357
10 Jansson J, Palmqvist A E C, Fridell E, Skoglundh M, Osterlund L, Thormahlen P, Langer V. *J Catal*, 2002, **211**: 387
11 Yu Y, Takei T, Ohashi H, He H, Zhang X, Haruta M. *J Catal*, 2009, **267**: 121
12 Benjaramtg M R, Katta L. *Chin J Catal* (催化学报), 2011, **32**: 800
13 Kim M H, Kim D W, Gode T. *Chin J Catal* (催化学报), 2011, **32**: 762
14 Qiao B, Wang A, Lin J, Li L, Su D, Zhang T. *Appl Catal B*, 2011, **105**: 103
15 Hu L H, Sun K Q, Peng Q, Xu B Q, Li Y D. *Nano Res*, 2010, **3**: 363
16 Tian B Z, Liu X Y, Yang H F, Xie S H, Yu C Z, Tu B , Zhao D Y. *Adv Mater*, 2003, **15**: 1370
17 Yang L X, Zhu Y J, Li L, Zhang L, Tong H, Wang W W, Cheng G F, Zhu J F. *Eur J Inorg Chem*, 2006, **2006**: 4787
18 Zhao Z G, Geng F X, Bai J B, Cheng H M. *J Phys Chem C*, 2007, **111**: 3848
19 Qiao R, Zhang X L, Qiu R, Kim J C, Kang Y S. *Chem Eur J*, 2009, **15**: 1886
20 Zheng J, Liu J, Lv D P, Kuang Q, Jiang Z Y, Xie Z X, Huang R B, Zheng L S. *J Solid State Chem*, 2010, **183**: 600
21 Chen A, Peng X, Koczkur K, Miller B. *Chem Commun*, 2004: 1964
22 Zhang H, Yang D, Ji Y J, Ma X Y, Xu J, Que D L. *J Phys Chem B*, 2004, **108**: 3955
23 Sun C W, Sun J, Xiao G L, Zhang H R, Qiu X P, Li H, Chen L Q. *J Phys Chem B*, 2006, **110**: 13445
24 Zhong L S, Hu J S, Liang H P, Cao A M, Song W G, Wan L J. *Adv Mater*, 2006, **18**: 2426
25 Zhong L S, Hu J S, Cao A M, Liu Q, Song W G, Wan L J. *Chem Mater*, 2007, **19**: 1648
26 Bain S W, Ma Z, Cui Z M, Zhang L S, Niu F, Song W G. *J Phys Chem C*, 2008, **112**: 11340
27 Cao C Y, Cui Z M, Chen C Q, Song W G, Cai W. *J Phys Chem C*, 2010, **114**: 9865
28 Cao C Y, Guo W, Cui Z M, Song W G, Cai W. *J Mater Chem*, 2011, **21**: 3204
29 Zeng S, Tang K, Li T, Liang Z, Wang D, Wang Y, Qi Y, Zhou W. *J Phys Chem C*, 2008, **112**: 4836
30 Long M, Cai W M, Cai J, Zhou B X, Chai X Y, Wu Y H. *J Phys Chem B*, 2006, **110**: 20211
31 Guttel R, Paul M, Schuth F. *Chem Commun*, 2010, **46**: 895